

Magnetohydrodynamic turbulence in supernova remnants

Nirupam Roy ^{1*}, Somnath Bharadwaj ^{2*}, Prasun Dutta ^{2*} and Jayaram N. Chengalur ^{1*}

¹NCRA-TIFR, Post Bag 3, Ganeshkhind, Pune 411 007, India

²Department of Physics and Meteorology & Centre for Theoretical Studies, IIT Kharagpur, Kharagpur 721 302, India

Accepted yyyy month dd. Received yyyy month dd; in original form yyyy month dd

ABSTRACT

We present estimates of the angular power spectra of the synchrotron radiation intensity fluctuations at 6 and 20 cm for the shell type supernova remnant Cas A and the filled-centre Crab supernova remnant. We find that the intensity fluctuations of both sources have a power law power spectrum with index -3.24 ± 0.03 . This power law power spectrum is consistent with the magnetohydrodynamic turbulence in the synchrotron emitting plasma. For Cas A, there is a break in the power spectrum and the power law index changes from -3.2 to -2.2 at large angular scale. This transition occurs at an angular scale that corresponds to the shell thickness of Cas A. We interpret this as a transition from three dimensional turbulence to two dimensional turbulence on scales that are respectively smaller and larger than the shell thickness.

Key words: MHD — ISM: general — ISM: individual (Cas A, Crab Nebula) — supernova remnants — turbulence

1 INTRODUCTION

Supernovae and supernova remnants play a very important role in astrophysics at the galactic scale. They cause the heating of the interstellar medium, acceleration of cosmic rays and enrichment of the interstellar medium with heavy elements created in the stellar core or in the supernova explosion. The shock wave traveling through the interstellar medium may also cause the gas clouds to collapse to form new stars. Thus, they work as a link between the gaseous and stellar components of the Galaxy. Based on their large scale structure, supernova remnants are broadly classified into three types: shell-type remnants, filled-centre remnants (or plerions) and composite remnants (Weiler & Sramek 1988). In addition to the large scale shell-like or filled-centre structures, all these remnants show a very rich and complicated structure over a wide range of scale and frequency of observation.

Although there have been many high resolution and high sensitivity multiwavelength observations of Galactic supernova remnants, there has not been, to the best of our knowledge, any systematic study to quantify the fine scale structure. Here we present 6 and 20 cm observations and estimates of the angular power spectra of the intensity fluctuation over a wide range of angular scales for the supernova remnants Cas A and the Crab Nebula.

The Crab Nebula (G184.6–5.8) is a supernova remnant and pulsar wind nebula in the constellation of Taurus in the third Galactic quadrant. It is a filled-centre nebula, $7' \times 5'$ in size (van den Bergh 1970) at a distance of approximately 2 kpc

(Trimble 1973). The remnant is of the famous supernova of 1054 AD and the Crab pulsar is observed to be at the centre of this nebula. At radio wavelengths the source is quite strong with a flux density of 1040 Jy at 1 GHz and, beside its filled centre structure, shows faint jet or tube like extension from the north edge of the remnant. Cassiopeia A or Cas A (G111.7–2.1) is in the constellation Cassiopeia in the second Galactic quadrant. This is a shell type supernova remnant of diameter $5'$ at a distance of approximately 3.4 kpc (Reed et al. 1995). The shell thickness estimated from the radial brightness profile at radio wavelengths is found to be approximately $30''$. At these wavelengths, it shows a clear shell like structure with compact emission knots and is one of the strongest radio sources in the sky with a flux density of 2720 Jy at 1 GHz. It is most probably the remnant of a late 17th century supernova (Fesen et al. 2006). There is some spectroscopic evidence that Cas A was a type IIb supernova (Krause et al. 2008). More details of both these supernova remnants can be found in the Galactic supernova remnants catalogue (Green 2004)¹.

At radio wavelengths, the dominant contribution to the supernova remnants' emission comes from the synchrotron radiation emitted by the relativistic electrons in the presence of magnetic fields. The observed structures over a wide range of scales are most probably result of the magnetohydrodynamic turbulence in the emitting plasma. Since the synchrotron radiation intensity fluctuation will depend on fluctuation of both density and magnetic field strength, it is expected that the power spectrum will reveal interesting information about the density and magnetic field fluctuation as well as about the nature of the turbulence in the plasma.

* E-mail: nirupam@ncra.tifr.res.in (NR); somnath@cts.iitkgp.ernet.in (SB); prasun@cts.iitkgp.ernet.in (PD); chengalu@ncra.tifr.res.in (JNC)

¹ See <http://www.mrao.cam.ac.uk/surveys/snr/s/> for an updated version.

We present here the estimates of the power spectrum obtained directly from the interferometric measurements of the visibility function of the sources. The analysis technique is briefly described below in §2. In §3, the details of the observational data and the results are given. Finally, we summarize and present our conclusions in §4.

2 ANALYSIS TECHNIQUE

Assuming that the angular extent of the source is small, the angular power spectrum, $P(u, v)$, of the intensity fluctuation of synchrotron radiation $\delta I(l, m)$ can be written as

$$P(u, v) = \int \int \xi(l, m) e^{-2\pi i(ul+vm)} dldm \quad (1)$$

where (l, m) is the direction on the sky, (u, v) is the inverse angular separations and ξ is the autocorrelation function of the intensity fluctuation

$$\xi(l - l', m - m') = \langle \delta I(l, m) \delta I(l', m') \rangle. \quad (2)$$

Here the angular brackets imply an average across different positions and directions on the sky. If the angular extent of the source is not small enough then, instead of taking the Fourier transform, a spherical harmonic decomposition of the autocorrelation function is to be done to get the angular power spectrum. Throughout this analysis, it is assumed that the angular size of the source is small and the statistical properties of the small scale intensity fluctuations are homogeneous and isotropic. Hence, the intensity fluctuation power spectrum $P(u, v)$ is a function of the magnitude $U = \sqrt{u^2 + v^2}$ only and is independent of the direction.

Since the complex visibility function $V(u, v)$ measured by an interferometer is the Fourier transform of the source brightness distribution $I(l, m)$,

$$V_s(u, v) = \int \int I(l, m) e^{-2\pi i(ul+vm)} dldm \quad (3)$$

where (u, v) is the baseline or the projected antenna separation in units of the wavelength of observation and is associated with an inverse angular scale, one can estimate the angular power spectrum directly from the measured visibility function. It can be easily shown that the squared modulus of the visibility is a direct estimator of the intensity fluctuation power spectrum

$$P(u, v) = \langle V_s(u, v) V_s^*(u, v) \rangle \quad (4)$$

where the angular brackets denote an average over all possible orientations of the baselines.

This method for estimating the power spectrum from the complex visibility function has been used earlier by Crovisier & Dickey (1983) and Green (1993). The technique of direct visibility based estimation of power spectrum has also been used and discussed in literature in various contexts like the analysis of interferometric observations of the Cosmic Microwave Background Radiation (e.g. Hobson et al. 1995), the large-scale H I distribution at high redshifts (Bharadwaj & Sethi 2001) and the interferometric H I observations to detect the epoch of reionization (Morales & Hewitt 2004; Bharadwaj & Ali 2005). The technical issues like the effect of the window function corresponding to the size of the source on the power spectrum estimator and the method of avoiding the noise bias by correlating the visibilities at two different baselines are described in detail in Begum et al. (2006). The actual algorithm of

Table 1. Details of the VLA and the GMRT data

Source	Wavelength	Array	Project	Date of observation
The VLA archival data:				
Cas A	6 cm	A	AR0435	09 Dec., 2000
Cas A	6 cm	A	AR0435	10 Dec., 2000
Cas A	6 cm	B	AR0435	25 Mar., 2001
Cas A	6 cm	B	AR0435	29 Apr., 2001
Cas A	6 cm	C	AR0435	25 Apr., 2000
Cas A	6 cm	D	AR0435	07 Sep., 2000
Crab	6 cm	A	AH0337	19 Oct., 1988
Crab	6 cm	A	AH0337	08 Nov., 1988
Crab	6 cm	B	AB0876	09 Aug., 1998
Crab	6 cm	C	AB0876	27 Jan., 1999
Crab	6 cm	D	AH0625	19 Nov., 1997
The GMRT data:				
Cas A	20 cm	–	11NRb02	03 Dec., 2006

estimating the power spectrum from the measured visibility function is outlined in Dutta et al. (2008). Here, a very similar algorithm, slightly modified to further reduce the noise bias, is used for the present work. To minimize the contribution of correlated noise power to the power spectrum estimator, visibilities are correlated at two different baselines with slightly different time-stamp for which the noise is expected to be uncorrelated. Begum et al. (2006) has shown that the real part of the measured visibility correlation directly estimates the power spectrum at baselines large compared to the inverse angular size of the source and at smaller baselines the true power spectrum is convolved with the window function. The error of the power spectrum is estimated accounting for both the noise in the measured visibility function and the finite number of independent estimates of the true power spectrum (cosmic variance).

3 DATA AND RESULTS

3.1 Summary of the data

The Giant Metrewave Radio Telescope (GMRT; Swarup et al. 1991) L-band (20 cm) receiver was used to observe the supernova remnant Cas A. The unique hybrid array configuration of the GMRT allows one to probe structures on both large and small angular scale in a single observation. Scans on standard calibrators were used for flux calibration, phase calibration and also to determine the bandpass shape. The Very Large Array (VLA) archival C-band (6 cm) data are also used for both the supernova remnant Cas A and Crab Nebula. A summary of the GMRT and the VLA data used for this work with the observation band, the telescope array configuration, the original programme code and the dates of observation is given in Table (1). Data analysis was carried out using standard AIPS. After flagging out bad data, the flux density scale and instrumental phase were calibrated. The calibrated visibility data of the target sources are then used to estimate the angular power spectra and the errors.

3.2 Results for Crab Nebula and Cas A

For the Crab Nebula, the angular power spectrum as a function of inverse angular scale is found to be power law with a power law index of -3.24 ± 0.03 . Since the effect of the convolution with the window function is more significant in the shorter baselines,

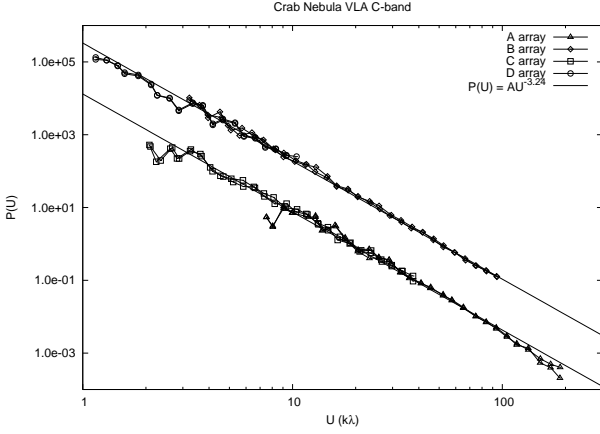


Figure 1. Intensity fluctuation power spectra for the Crab Nebula. The data points are from the VLA 6 cm (C-band) observation with different array configurations and at two different IFs. The line is the best fit power law with the power law index of -3.24 . Data from different array configuration and the best fit power law are shown here with an offset in amplitude for clarity.

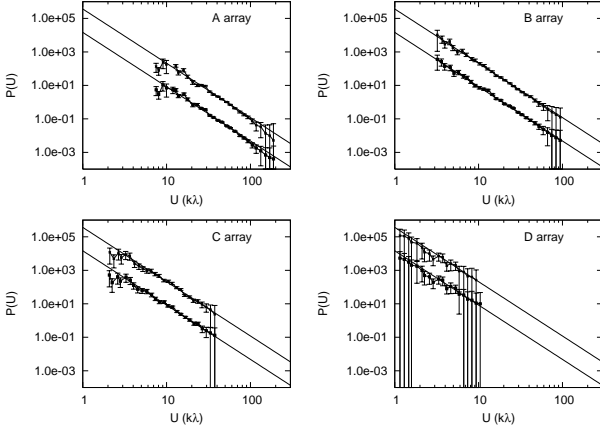


Figure 2. Intensity fluctuation power spectra with $\pm 1\sigma$ errorbars for the Crab Nebula. The VLA 6 cm (C-band) power spectra derived from the observation with different array configurations are shown in different panels. Results from two different IFs are plotted in the same panel with an offset in amplitude. The line is same as in Figure (1).

the power law index is extracted by fitting the power spectra in the longer baseline range of $6 - 60$ k λ . Figure (1) shows the spectra derived from the VLA 6 cm observation with different array configuration and at two different intermediate frequencies (IFs). The best fit power law, with an offset introduced in amplitude for clarity, is also shown in the same figure. The four panels in Figure (2) show the power spectra with $\pm 1\sigma$ errorbars derived using the data from different VLA array configuration and IFs. The noise in the measured visibility function dominates at long baselines and the cosmic variance is the significant source of error at small baselines. It is clear from these figures that for a wide range of scales (about $1 - 100$ k λ which corresponds to an angular scale of $2.5 - 250$ arcsec), the intensity fluctuation angular power spectra is a power law function of inverse angular scale. The power spectra derived from data from different array configurations and different IFs are in very good agreement.

The power spectrum for Cas A is also found to be a power law

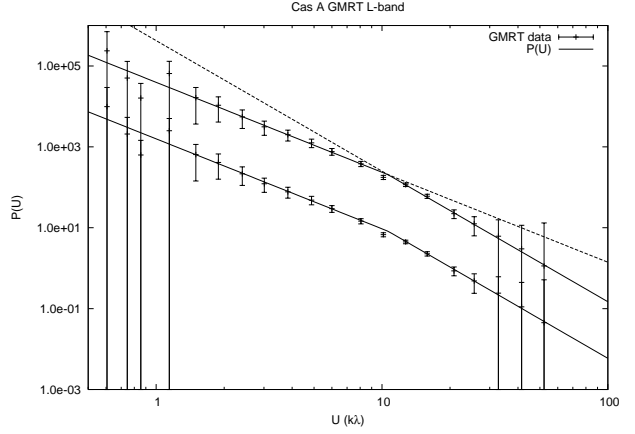


Figure 3. Intensity fluctuation power spectra for the supernova remnant Cas A. The points with $\pm 1\sigma$ errorbars are from the GMRT 20 cm (L-band) data with two different observation frequencies. The line is showing the best fit power law with power law index of -2.22 and -3.23 before and after the break (at 10.6 k λ) respectively. Power spectra derived from different frequency ranges and the best fit function are plotted with an offset in amplitude.

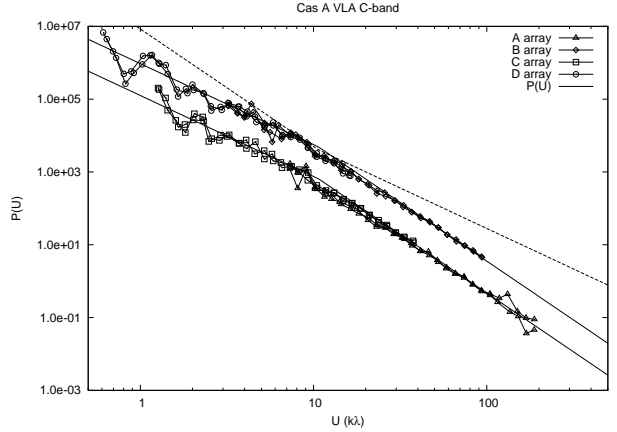


Figure 4. Intensity fluctuation power spectra for Cas A. The data points are from the VLA 6 cm (C-band) observation with different array configurations and at two different IFs. The line is the best fit function as in Figure (3). Data from different array configuration and the best fit function are shown here with an offset in amplitude.

with a very similar power law index at small angular scales. But, as shown in Figure (3), there is a break in the spectrum at about 10.6 k λ (~ 25 arcsec) and the power law index changes significantly at smaller U . The best fit power law function for the power spectrum derived from the GMRT 20 cm data has a power law index of -2.22 ± 0.03 in the shorter baseline range ($1.6 - 10$ k λ). After the break the index changes to -3.23 ± 0.09 (estimated from the range $11 - 30$ k λ) and the power spectrum remains steeper all the way up to the smallest angular scale (~ 5 arcsec) probed in this observation. These results for Cas A power spectrum are consistent with the power spectra derived from the VLA 6 cm archival data of Cas A. It is found that the 6 cm power spectrum is also a broken power law with the same power law index and the break at the same angular scale as in the 20 cm power spectrum. The VLA 6 cm power spectra obtained from observation with different array configurations and two different IFs are plotted in Figure (4). This

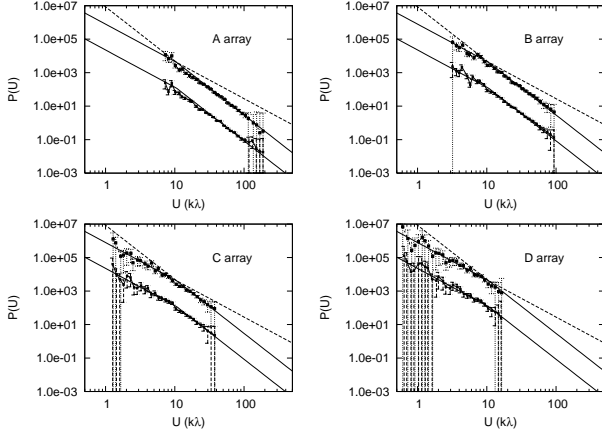


Figure 5. Intensity fluctuation power spectra with $\pm 1\sigma$ errorbars for Cas A. The VLA 6 cm (C-band) power spectra derived from the observation with different array configurations are shown in different panels. Results from two different IFs are plotted in the same panel with an offset in amplitude. The line is same as in Figure (3).

shows that the steeper power law at the long baseline range is in fact extended upto $100\text{ k}\lambda$ ($\sim 2.5\text{ arcsec}$). The four panels in Figure (5) show the power spectra with $\pm 1\sigma$ errorbars derived using the data from four different VLA array configuration and two IFs. Clearly, for Cas A also, the power spectra derived from 20 cm and 6 cm data with different array configurations and different IFs are in good agreement.

3.3 Interpretation of the results

The power law index of the steeper part of the Cas A angular power spectrum is completely consistent, within the measurement errorbars, with the power law index of the Crab Nebula power spectra. The break in the Cas A power spectrum and the change of the power law index at small baseline range (or large angular scale) is very interesting. We have verified analytically that the shell type geometry of Cas A will affect the power spectrum significantly only at very small U by convolving it with a window function which is the Fourier transform of the two dimensional projection of this optically thin shell. The same is also true for the optically thin spherical geometry of the Crab Nebula. For the long baseline range around $10\text{ k}\lambda$, the effect will be negligible and can not explain the sharp break and the significant change of power law index by ~ 1 . It appears that a plausible explanation is a transition from three dimensional at small scales ($U > 10\text{ k}\lambda$) to two dimensional turbulence at large scales ($U < 10\text{ k}\lambda$). The shell thickness sets the angular scale of the transition. On length scales smaller than the shell thickness, the shell can have modes of perturbation in all three independent directions. But on length scales larger than the shell thickness, there will be no modes perpendicular to the shell thickness. This makes the turbulence to change from a three dimensional to effectively a two dimensional in nature and hence the power law index changes by 1. This change in slope may possibly be related to the fact that the slope of the velocity power spectrum changes from $-11/3$ to $-8/3$ in going from 3D to 2D for incompressible, Kolmogorov turbulence (Kolmogorov 1941). The density power spectrum is predicted to follows the velocity power spectrum in the Goldreich & Sridhar (1995) model of MHD turbulence. The observation, that the angular scale of this break matches approximately with the shell thickness, is indicative of the consistency of

this picture. A similar difference of ≈ 1 in the power law index has also been observed and interpreted as a transition from three dimensional turbulence to two dimensional turbulence in the power spectrum of H I 21 cm emission intensity fluctuations of the Large Magellanic Cloud (Elmegreen et al. 2001) and the galaxy NGC 628 (Dutta et al. 2008).

The scale-free nature of the power spectra over a wide range of scales and a very similar value of the power law index for power spectra of two very different type of supernova remnants suggests the universality of the physical process responsible for the observed intensity fluctuation. We propose that the fluctuation is most probably due to the turbulence in the synchrotron emitting plasma that gives rise to the power law power spectrum. The interaction of the propagating shock with the turbulent interstellar medium is known to enhance the turbulence in the postshock region and causes the spatial variation of emission in supernova remnants (Balsara et al. 2001). We investigate here whether the observed power spectrum $P(k) \propto k^{-3.2}$, or equivalently the energy spectrum $E(k) = k^2 P(k) \propto k^{-1.2}$, is consistent with our present understanding of astrophysical turbulence. The observed intensity fluctuation power spectra is related to the density and magnetic field power spectra which, in turn, are found, from numerical simulations, to closely follow the velocity fluctuation power spectra. For incompressible and nonmagnetized turbulence Kolmogorov theory suggests an isotropic power law velocity fluctuation energy spectrum $E_v(k) \propto k^{-5/3}$ where k is the magnitude of the wave vector (Kolmogorov 1941). Iroshnikov (1964) and Kraichna (1965) gave a model of magnetic incompressible turbulence (IK theory) that predicts, even in the presence of magnetic field, isotropic power law energy spectra $E(k) \propto k^{-3/2}$ for both velocity and magnetic field. Without any assumption of isotropic energy distribution, Goldreich & Sridhar (1995) proposed a model of incompressible magnetohydrodynamic turbulence that predicts a Kolmogorov-like energy spectra $E_v(k_\perp) \propto k_\perp^{-5/3}$ where k_\perp is the component of the wave vector perpendicular to the local magnetic field direction. It also predicts an anisotropy condition $k_\parallel \propto k_\perp^{2/3}$ where k_\parallel is the component of the wave vector parallel to the local magnetic field direction. But, even if there is anisotropy in the system of reference defined by the local magnetic field, it is worth keeping in mind that there will only be moderate anisotropy in the observer's reference.

For compressible magnetohydrodynamics turbulence, there is, unfortunately, no widely-accepted theory and much of the present understanding has come from numerical results. Recent numerical simulation indicates that, for compressible magnetohydrodynamic turbulence, both the velocity and magnetic field energy spectra and anisotropy in Alfvén modes and slow modes are as predicted by (Goldreich & Sridhar 1995). But the energy spectra for fast modes are isotropic and the scaling is as predicted in IK theory (Cho & Lazarian 2002b). It is also found that, at least in case of incompressible magnetic turbulence, viscous damping on scales larger than the magnetic diffusion scale can make the magnetic energy spectrum significantly less steep. Cho et al. (2002) reports magnetic energy spectrum $E_b(k) \propto k^{-1}$ implying rich structure of magnetic field on small scales.

The synchrotron emissivity $i_s \propto n_e |B_\perp|^{(p+1)/2}$ where n_e is the electron number density, B_\perp is the magnetic field component perpendicular to the line of sight and the typical value of the power law index p of electron energy distribution in supernova remnants is about 2 (Green 1991). One dimensional numerical analysis suggests that if the magnetic field power spectrum is a power law, then $|B|^{(p+1)/2}$ will also have a power law spectrum with the same in-

dex for the values of p in the range of our interest. But, because of this nonlinearity, in general it is not straightforward to derive the magnetic field fluctuation power spectrum from the intensity fluctuation power spectrum. It is also not necessarily true that the density distribution and magnetic field are strongly coupled. Numerical simulation and analytical study in fact suggest that in compressible magnetohydrodynamic turbulence, the magnetic field strength and density are only weakly correlated (Passot & Vázquez-Semadeni 2003). Beresnyak et al. (2005) also reports a flat and isotropic density spectrum from numerical simulation of supersonic magnetohydrodynamic turbulence. But, if the electron density distribution smoothly follows the magnetic field inhomogeneities in the supernova remnants, the synchrotron intensity fluctuation power spectrum is directly related to the magnetic field power spectrum. In this condition, following the analysis of Deshpande et al. (2000), one can conclude that if the intensity fluctuation has a power law power spectrum then the magnetic field fluctuation will also have a power law spectrum with the same power law index, provided that the magnetic field perturbation amplitude is small. The effect of the nonlinear law of synchrotron emission on the power spectrum is not clear in situations when the perturbation amplitude is high or correlation between the magnetic field strength and density is weak.

The observed intensity fluctuation power spectrum is somewhat shallower than the expected spectrum of the magnetic field. From the above discussion, one can identify three plausible reasons for this discrepancy which can make the spectrum less steep. They are (i) viscous damping on scales larger than the magnetic diffusion scale, (ii) weak or no correlation between the magnetic field and the density distribution and (iii) large amplitude of magnetic field perturbation which may affect via the nonlinearity of synchrotron emissivity.

Interestingly, numerical, observational and theoretical studies of synchrotron emission fluctuations are carried out in a completely different context to understand the effect of the Galactic foreground emission on the angular power spectrum of the cosmic microwave background (see Cho & Lazarian 2002a, and references therein for details) and in some of the cases the intensity fluctuations are attributed to turbulence (Chepurnov 1998; Tegmark et al. 2000; Cho & Lazarian 2002a). Though in a very different range of angular scale, the energy spectrum of the Galactic synchrotron foreground is found to be a range of power laws with power law index ~ -1 for higher latitudes (Cho & Lazarian 2002a, and references therein). This is less steep than the expected $k^{-5/3}$ energy spectrum of the magnetic field. Clearly, a similar discrepancy is evident in this case also. But, in spite of this discrepancy, one can say that the near-Kolmogorov power law power spectrum is broadly consistent with our present understanding of the magnetohydrodynamic turbulence.

4 CONCLUSIONS

We have analysed the data from GMRT 20 cm and VLA 6 cm observations of two supernova remnants Cas A and Crab Nebula and estimated the angular power spectra of the synchrotron radiation intensity fluctuation over a wide range of angular scale. We report, for the first time, a power law power spectrum of the synchrotron radiation intensity fluctuation in supernova remnants. The power law index is found to be -3.24 ± 0.03 for both these sources with very different large scale morphology. For Cas A, there is a break in the power spectrum and the power law index changes from -3.2

to -2.2 at angular scale larger than the size of the shell thickness. This change is a result of the anisotropy of the perturbation at length scales larger than the shell thickness. This power law power spectrum is consistent with our present understanding of the magnetohydrodynamic turbulence derived mostly from existing numerical simulation results.

ACKNOWLEDGMENTS

This research has made use of the NASA's Astrophysics Data System, the National Radio Astronomy Observatory (NRAO) VLA archival data and data from the GMRT observation. The NRAO is a facility of the National Science Foundation operated under cooperative agreement by Associated Universities, Inc. We thank the staff of the GMRT who have made these observations possible. The GMRT is run by the National Centre for Radio Astrophysics of the Tata Institute of Fundamental Research. NR would like to acknowledge the hospitality of all the staff members of the Centre for Theoretical Studies (Indian Institute of Technology, Kharagpur) during his stay for this collaboration. We are grateful to Dipankar Bhattacharya, Dave Green, Ranjeev Misra, Rajaram Nityananda, Dmitri Pogossyan, A. Pramesh Rao and Kandaswamy Subramanian for much encouragement and many helpful comments. We are also grateful to the anonymous referee for useful comments.

REFERENCES

- Balsara D., Benjamin R. A., Cox D. P., 2001, *ApJ*, 563, 800
- Begum A., Chengalur J. N., Bhardwaj S., 2006, *MNRAS*, 372, L33
- Beresnyak A., Lazarian A., Cho J., 2005, *ApJ*, 624, L93
- Bharadwaj S., Ali S. S., 2005, *MNRAS*, 356, 1519
- Bharadwaj S., Sethi S. K., 2001, *JA&A*, 22, 293
- Chepurnov A. V., 1998, *Astron. Astrophys. Trans.*, 17, 281
- Cho J., Lazarian A., 2002a, *ApJ*, 575, L63
- Cho J., Lazarian A., 2002b, *Phys. Rev. Lett.*, 88, 245001
- Cho J., Lazarian A., Vishniac E. T., 2002, *ApJ*, 566 L49
- Crovisier J., Dickey J. M., 1983, *A&A*, 122, 282
- Deshpande A. A., Dwarakanath K. S., Goss W. M., 2000, *ApJ*, 543, 227
- Dutta P., Begum A., Bharadwaj S., Chengalur J. N., 2008, *MNRAS*, 384, L34
- Elmegreen B. G., Kim S., Staveley-Smith L., 2001, *ApJ*, 548, 749
- Fesen R. A., Hammell M. C., Morse J., Chevalier R. A., Borkowski K. J., Dopita M. A., Gerardy C. L., Lawrence S. S., Raymond J. C., van den Bergh S., 2006, *ApJ*, 645, 283
- Goldreich P., Sridhar S., 1995, *ApJ*, 438, 763
- Green D. A., 1991, *PASP*, 103, 209
- Green D. A., 1993, *MNRAS*, 262, 327
- Green D. A., 2004, *Bull. Astron. Soc. India*, 32, 335
- Hobson M. P., Lasenby A. N., Jones M., 1995, *MNRAS*, 275, 863
- Iroshnikov P., 1964, *Sov. Astron.*, 7, 566
- Kolmogorov A., 1941, *Dokl. Akad. Nauk SSSR*, 31, 538
- Krause O., Birkmann S. M., Usuda T., Hattori T., Goto M., Rieke G. H., Misselt K. A., 2008, *Science*, 320, 1195
- Kraichnan R., 1965, *Phys. Fluids*, 8, 1385
- Morales M. F., Hewitt J., 2004, *ApJ*, 615, 7
- Passot T., Vázquez-Semadeni E., 2003, *A&A*, 398, 845
- Reed J. E., Hester J. J., Fabian A. C., Winkler P. F., 1995, *ApJ*, 440, 706

- Tegmark M., Eisenstein D. J., Hu W., de Oliveira-Costa A., 2000, ApJ, 530, 133
Trimble V., 1973, PASP, 85, 579
Swarup G., Ananthakrishnan S., Kapahi V. K., Rao A. P., Subrahmanya C. R., Kulkarni V. K., 1991, Curr. Sci., 60, 95
van den Bergh S., 1970, ApJ, 160, L27
Weiler K. W. & Sramek R. A., 1988, ARA&A, 26, 295

This paper has been typeset from a $\text{T}_{\text{E}}\text{X}/\text{L}^{\text{A}}\text{T}_{\text{E}}\text{X}$ file prepared by the author.